

MARS SCIENCE LABORATORY ORBIT DETERMINATION DATA PRE-PROCESSING

Eric D. Gustafson^{*}, Gerhard L. Kruizinga[†], and Tomas J. Martin-Mur[‡]

The Mars Science Laboratory (MSL) was spin-stabilized during its cruise to Mars. We discuss the effects of spin on the radiometric data and how the orbit determination team dealt with them. Additionally, we will discuss the unplanned benefits of detailed spin modeling including attitude estimation and spacecraft clock correlation.

INTRODUCTION

The Mars Science Laboratory (MSL), carrying the Curiosity rover, was spin-stabilized during its cruise to Mars, just like the two Mars Exploration Rover spacecraft preceding it. Spin-stabilization provides many advantages that simplify cruise operations, but it adds complexity to the radiometric data used for navigation. This paper discusses the effects of spin on orbit determination (OD) and how the MSL (OD) team dealt with them. We will also discuss the unplanned benefits of high-fidelity spin modeling.

We will briefly cover the theoretical background on how a circularly-polarized radio signal transmitted from a spinning spacecraft differs from one transmitted from a non-rotating antenna. In summary, the spin produces two main effects: a periodic signature and a frequency bias.

Previous missions have taken different approaches dealing with these effects. One straightforward approach, used during launch on MER-A,¹ was to simply ignore the periodic signature and treat the signal as if it were emanating from the spacecraft center of mass. This has the significant downside that the data must be de-weighted because the periodic signature can be over two orders of magnitude larger than the 2-way Doppler noise. Another approach was used during MER-B launch and on both MER spacecraft during cruise: compress the data using a count time that is as close as possible to an integer multiple of the period. If the count time is an exact multiple of the spin period, then this approach completely removes the periodic signature, leaving only a frequency bias. The drawback is that any mismatch between the period multiple and the count time leaves a long-period signature in the data.

A third, and more direct, technique was used by the Mars Observer, Genesis, and MER missions. These missions used the Doppler data to estimate parameters of a sinusoid, then subtracted it from

^{*}MSL Orbit Determination Analyst; Mission Design and Navigation Section; Jet Propulsion Laboratory, California Institute of Technology, 4800 Oak Grove Drive, Pasadena, California 91109.

[†]MSL Orbit Determination Lead; Mission Design and Navigation Section; Jet Propulsion Laboratory, California Institute of Technology, 4800 Oak Grove Drive, Pasadena, California 91109.

[‡]MSL Navigation Team Chief; Mission Design and Navigation Section; Jet Propulsion Laboratory, California Institute of Technology, 4800 Oak Grove Drive, Pasadena, California 91109.

the data. MER and Genesis² took a purely geometrical approach by estimating the amplitude, frequency, phase and bias independently. Mars Observer³ took a more physical approach by estimating the spin period, projected distance between the antenna and spin axis, and spin phase. The amplitude was properly correlated with the period—the lower the period, the faster the antenna velocity and the larger the amplitude of the Doppler signature. Mars Observer also computed the Doppler bias from the spin rate.

Although these methods were successful on their respective missions, MSL chose yet another method in order to meet the stringent OD accuracy requirements⁴ for precision landing on Mars: explicitly modeling the rotational motion of the spacecraft. The rotational estimation was performed as a pre-processing step before orbit determination, and came to be called “despinning.” During despinning, the raw high-rate tracking data received from the rotating antenna were modified to be representative of the non-rotating center of mass of the spacecraft. Once that was accomplished, the data could be compressed without any loss of information. This allowed for significant OD computational time savings over simultaneously estimating both the spin and trajectory states. The attitude estimation was not sensitive to disturbances such as media, Earth orientation parameters, or even a moderate amount of trajectory error. This allows the OD analyst to despin the data once, compress it, then use that data set for all remaining trajectory estimation.⁵

ANTENNA MOTION AND CIRCULAR POLARIZATION

The rotation of the spacecraft imparts two effects on the Doppler data: a periodic signature associated with the antenna motion and a frequency bias due to the circular polarization.

The periodic signature is due simply to the physical movement of the antenna phase center along the line-of-sight to the receiving ground station. As expected for MSL, the nutation angle was always small during the mission, which meant the motion of the antenna with respect to the spacecraft center of mass is simple harmonic motion. Hence, the Doppler shift with respect to the center of mass can be written as

$$\Delta f = A \sin(\omega t + \theta) + b, \quad (1)$$

where A is the amplitude of the periodic signal, ω is the spacecraft spin rate, t is time, θ is the spin phase, and b is the frequency bias. The amplitude is governed by the distance between the spacecraft antenna phase center and the spin axis, the spin rate, and the angle between the Earth-CM line and the spacecraft spin axis.⁶

The frequency bias exists because a rotating antenna will increase or decrease the transmitted or received frequency of a circularly polarized signal by the spin rate of the antenna. Given a spin rate ω and including the two-way turnaround ratios, the two-way X-band frequency bias is

$$b = \omega \left(1 + \frac{880}{749} \right), \quad (2)$$

where 880/749 is the X-band turnaround ratio on the spacecraft transponder. For MSL, the nominal spin rate was 2 RPM, so the typical Doppler bias was about 72.5 mHz:

$$b = 2 \text{ RPM} \cdot \frac{1 \text{ Hz}}{60 \text{ RPM}} \cdot \left(1 + \frac{880}{749} \right) = 0.0725 \text{ Hz}.$$

For reference, a typical standard deviation of the post-fit Doppler residuals was just 3 mHz.

DESPINNING PROCESS

We will describe the despin process from two perspectives: a top-down view relevant to the end-user, and a bottom-up view of the underlying software implementation.

Starting with the underlying implementation, the despin process can be separated into two distinct subprocesses. First is the “heuristic,” which needs no initial guess of spin state as input, and whose output is a coarse spin state estimate. Second is the “despin filter,” which does require an initial spin state of reasonable fidelity, but produces a very accurate estimate of the spin state.

Heuristic

Fundamentally, the estimation of frequency is a nonlinear problem because sinusoids of different frequencies are orthogonal to each other. This only holds over infinite durations, and for finite intervals, there will always be a small frequency region where linearity remains valid. Currently, the JPL navigation software Monte⁷ uses a linear filter. The heuristic is the method by which the linear filter can solve a nonlinear problem. This is accomplished by providing the filter with an initial guess sufficiently close to the truth such that the problem remains in the small linear regime.

The algorithms used by the heuristic are based on frequency analysis of axially-symmetric rigid-body motion.⁸ Before MSL launched, heuristic performance was tested extensively on actual tracking data from the MER-B spacecraft. The Juno mission, launched on August 5, 2011, was actually the first to use this tool operationally.*

The inputs to the heuristic are tracking data, spacecraft antenna location, spacecraft trajectory, spin axis orientation, and spacecraft inertia values. No information on the spin state is necessary. The first step in the heuristic is a fast Fourier transform (FFT) to determine the spin rate. Then, a tailored nonlinear search over the remaining space finds suitable values for spin phase, precession rate and phase, nutation angle, and the distance of the antenna from the spin axis.

Despin Filter

The despin filter is the process that takes a rough spin state estimate and refines it to the accuracy needed by orbit determination. The initial estimate can come from the heuristic, or simple linear propagation of a previous spin state. During MSL operations, preference was always to attempt propagating the previous spin state unless a known event would cause that state to be unpredictable, e.g., propulsive events or HRS maintenance. As with the heuristic, the despin filter was tested on MER-B data and used operationally on Juno.

There are three frames relevant to the despinning process. First is the EME2000 frame, considered to be the inertial frame. From there, the “MSL Pole Frame” defined the direction of the angular momentum vector. Finally, the “MSL Inertia Frame” is the body-fixed frame aligned with the principle axes of inertia. The rotation from the Pole Frame to the Inertia Frame was defined as a 3-1-3 sequence of Euler rotations using the angles RA, DEC, and W, where RA is the right ascension, DEC is the declination, and W is the spin angle:

$$\vec{x}_{\text{Inertia Frame}} = R(t)\vec{x}_{\text{Pole Frame}}, \quad (3)$$

where

$$R(t) = R_z(W(t))R_x(\pi/2 - DEC(t))R_z(\pi/2 + RA(t)), \quad (4)$$

*MSL launched on November 26, 2011.

$$R_x(\alpha) = \begin{bmatrix} 1 & 0 & 0 \\ 0 & \cos(\alpha) & \sin(\alpha) \\ 0 & -\sin(\alpha) & \cos(\alpha) \end{bmatrix}, \quad (5)$$

and

$$R_z(\alpha) = \begin{bmatrix} \cos(\alpha) & \sin(\alpha) & 0 \\ -\sin(\alpha) & \cos(\alpha) & 0 \\ 0 & 0 & 1 \end{bmatrix}. \quad (6)$$

The nutation angle, ϕ , is related to *DEC* by

$$\phi = \pi/2 - DEC. \quad (7)$$

Table 1: Despin filter *a priori* sigmas

Parameter	<i>A priori</i> sigma
Inertia Frame / W[0]	30 deg
Inertia Frame / W[1]	0.14325 deg/sec
Inertia Frame / W[2]	4.0×10^{-9} deg/sec ²
Inertia Frame / RA[0]	30 deg
Inertia Frame / RA[1]	0.14325 deg/sec
Inertia Frame / RA[2]	4.0×10^{-9} deg/sec ²
Inertia Frame / DEC[0]	0.1 deg
DSN Two-way Doppler Bias	0.1 Hz
Antenna Cylindrical Radius	0.005 m
Pole Frame / RA[0]	5 deg
Pole Frame / DEC[0]	5 deg

A key filter input is the *a priori* uncertainty associated with each quantity to be estimated. Table 1 lists the *a priori* sigma associated with each estimated parameter. An angle followed by $[n]$ is the n -th derivative of that angle. For example, at the filter epoch, Inertia Frame / W[0] is the phase of the W angle and Inertia Frame / W[1] is the angular velocity.

The filter was typically ran three times, with each run being followed by a run of the autoeditor. The autoeditor performs three important tasks: outlier rejection and data editing, filter weight computation, and data classification. The editing algorithm is the “ n - σ ” algorithm, implemented as follows for a user-specified value of n :

1. Compute the mean and standard deviation of the valid data, m and σ .
2. Check the value, v , of each point; if v satisfies $m - n\sigma \leq v \leq m + n\sigma$, mark it as valid, otherwise mark it as ignored.
3. Return to Step 1 until the classification of valid/invalid points doesn't change or a maximum iteration limit is hit.

Before the filter was run for the first time, the data was edited at the 6 - σ level to remove any obvious outliers. Within the iteration loop, a 3 - σ value was used for more routine data editing.

The data weighting functionality of the autoeditor computes filter weights based on the standard deviation of the valid residuals. A scale factor of 3.36 was applied to the Doppler sigma to account

for solar plasma effects.⁹ A minimum sigma value was also specified to prevent the data from being trusted more than deemed reasonable.

The last important function of the autoeditor is data classification. All data was classified into “arcs.” Data arcs are defined such that all data within an arc is of the same type (Doppler or range), transmitting station, and receiving station. This is a more restrictive definition than classifying data “per-pass” because the passes were split into separate arcs if there was an impulsive event or spin state change. The despin filter solves for the spin state one arc at a time, independently from other arcs.

After the filter-autoeditor combination converged, the spin state estimation was finished. The most fundamental outputs of the filter are the estimated values and their associated uncertainty. The filter also created several plots used to verify the correctness of the solution. These outputs will be discussed in more detail in the results section.

At this point, the raw tracking data was modified to be representative of the non-rotating center of mass. This data could be used by the OD filter, however, the data were typically compressed to save OD computation time and memory. The Doppler data used in OD is the “differenced range” formulation, defined as the number of phase cycles during an interval divided by the duration of the interval. Interplanetary mission interval durations are usually on the order of minutes, that is, one Doppler data point every few minutes. Compared with MSL’s spin rate of 2 RPM, this data rate would make attitude estimation difficult because the sampling rate is well below the Nyquist rate. If the attitude were to be estimated concurrently with the trajectory, then high-rate Doppler data would be required. This would cause the OD process to be much slower and more data-intensive than previous missions. Fortunately, the attitude and trajectory are not tightly coupled, and estimating them independently was the approach taken throughout the mission.

End-User Interaction

The despin tools are designed to be highly automated and modular. This allows for straightforward usage during nominal situations, yet still allows the user to intervene at certain points if necessary. In fact, shortly after every DSN pass, an automated script would attempt to despin the data and email results to the OD team in a format easily checked on smartphones. This automated “quicklook” enabled near-realtime remote monitoring of the data. As long as there were no propulsive events or HRS maintenance, these automated despin solutions were very robust and would often be used to initialize the official despin solution.

A few auxiliary files were maintained by the users to control the overall setup and flow of the process. General inputs were defined in a file with similar structure to a FORTRAN namelist. Of course, since the despin tools are written in Python, this file simply contained Python-importable variable definitions used throughout the code. Another file was a list of “breakpoints,” which are times at which to force a new data arc. These breakpoints are used at any event that can abruptly change the spin state, for example, trajectory correction maneuvers or HRS maintenance. Lastly, the Arc Information File (AIF) stored the bookkeeping for all data. This stored arc start and end times, data type, spin state, ground stations, and more.

Each step in the despin procedure can be associated with a particular script as summarized by the following steps:

1. Initial setup. The user decides which OD solution to start from. This will define the overall

setup and the trajectory to be used for computing residuals during despinning.

2. Local data preparation. Copies the relevant raw, high-rate data to the local directory.
3. Data editing and classification. Perform $6\text{-}\sigma$ autoediting to remove “blunder points” and compute initial data weight. Also apply any manual edits and classify data into arcs.
4. Spin state initialization. This step is standard, but optional. If the automated quicklook for the data was successful, then the user would benefit from using the quicklook spin state as the initial spin state for the despin. If no explicit state is initialized, then the following step will automatically run the heuristic.
5. Despin. This is the main program. Run the heuristic as needed to obtain any spin states that haven’t already been initialized, then proceeds to run the despin filter on each arc.
6. Data merging. The despun data for each arc exists in separate subdirectories; this steps combines all data into one tracking file.
7. Data compression. Compress the despun Doppler data to the rate requested by the OD analysts.
8. Global data update. Once the despinner has verified the success of the process, the compressed despun data is merged with the global tracking data.

DESPINNING RESULTS

This section presents the outputs and typical results from the despin process. We start by discussing launch, which was a particularly interesting time for despinning because the DSN was using a cross-polarized link, the spin rate was changing, and the polarity was intentionally left unresolved to ensure we got the correct sign on the Doppler bias. Next, we discuss nominal cruise, which was much more routine.

Launch Despin

During the first DSN pass, the DSN intentionally used a cross-polarized receiver to limit the power into the sensitive station electronics. This caused the Doppler data to be noisy because when a circularly-polarized signal is reflected, its polarity reverses. Therefore, the DSN was not only receiving the attenuated signal from the spacecraft antenna, but also large amounts of unwanted multipath from spacecraft reflection. Figure 1 shows the despun Doppler residuals from the first pass. The boxed data were rejected automatically by the $3\text{-}\sigma$ autoeditor, leaving mostly the primary signal with nearly Gaussian residuals. It should be noted that the autoeditor’s $n\text{-}\sigma$ algorithm proved to be very robust and effective with this difficult data.

Shortly after MSL’s launch, periodic and secular changes in the spin rate were clearly detectable. Figure 2 shows the peak frequency vs. time for various data slices. More specifically, if a data point is plotted at time t for a window of dt , then the value being plotted is obtained by computing a Lomb-Scargle periodogram¹⁰ of the data between times $t - dt/2$ and $t + dt/2$, then picking the frequency that has the highest power content.

The oscillations, most evident in the 0.25 hour window, are thought to be result of non-rigid-body motion, perhaps fuel slosh. The secular spin acceleration is likely due to due to outgassing,

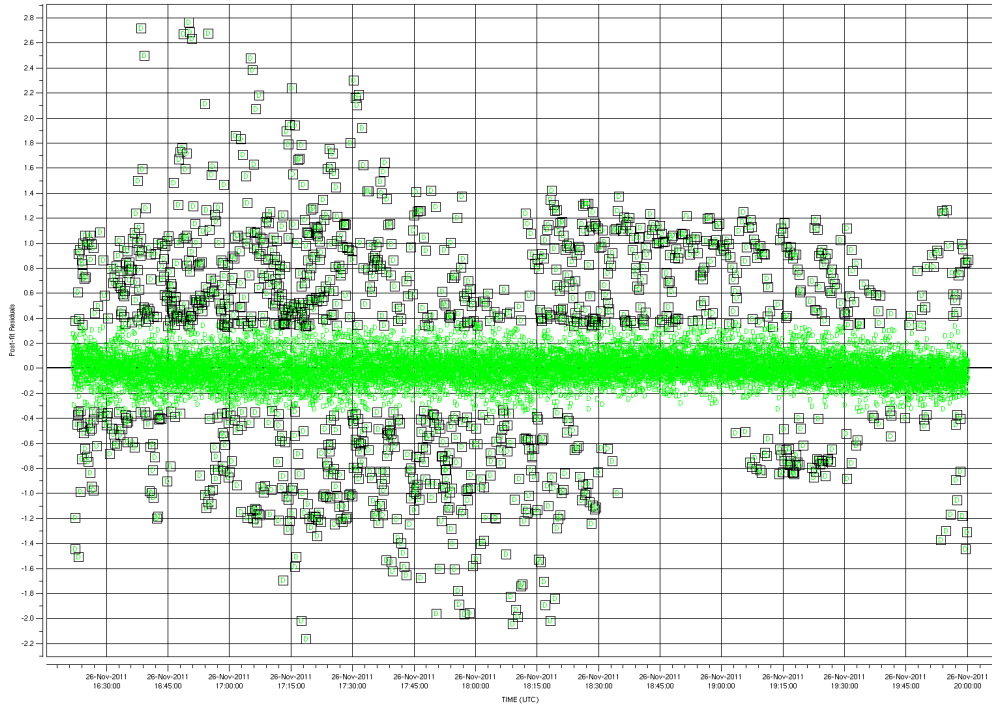


Figure 1: Launch cross-polarized residuals.

which would be consistent with acceleration estimates from OD.⁵ Even though the magnitude of this acceleration was about 3×10^{-10} deg/sec², it was clearly evident in the data. This supports the usefulness of radiometric data for means other than solely orbit determination.

The Doppler bias was estimated in the OD filter during launch to allow for confirmation or correction of signal polarization assumptions. Once enough range data was received, the OD bias estimate gave the correct polarization and bias.

Figure 3 is a plot of the despun residuals vs. phase angle of the spacecraft antenna. This is interesting because it shows a repeatable dependence of the residual on the spin angle of the antenna. This pattern is a characteristic of the low gain antenna (LGA). This beneficial byproduct of despining gives increased insight into the source of data noise – we can say that some source of Doppler noise is simply the line-of-sight motion of the LGA phase center.

Cruise Despin

The majority of DSN passes during cruise were straightforward from the despining perspective. The spin state could typically be initialized using the previous pass or automated quicklook, and there were rarely events that necessitated the use of breakpoints. This section will describe the outputs of the despin process for a representative pass on March 25, 2012, from about 08:00 to 15:00 UTC.

Table 2 gives representative post-fit sigma values of the parameters for a typical cruise pass. Since nutation was small during cruise ($DEC \approx \pi/2$), the intermediate rotation in Eq. (4) is nearly identity, so the first and third rotations are nearly along the same direction with respect to the Pole Frame. Therefore, the Inertia Frame / W[*] and Pole Frame / RA[*] estimates are nearly perfectly

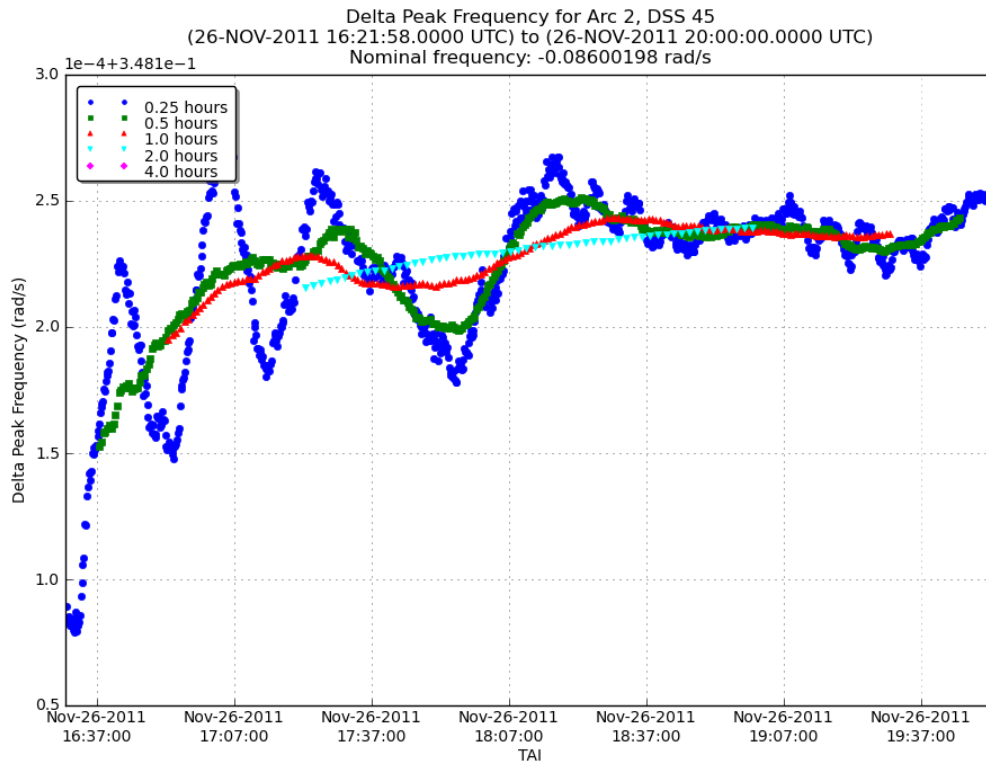


Figure 2: Launch frequency vs. time

correlated, and the reported sigma values are almost identical. The actual spin rate, used in the computation of the Doppler bias in Eq. (2), is computed as:

$$\omega = (\text{Inertia Frame} / W[1]) + (\text{Inertia Frame} / RA[1])$$

The raw “spinning” residuals are shown in Fig. 4, zoomed in to show the periodic signature. The despun residuals for the same data are shown in Fig. 5. The periodic signature visible in Fig. 4 is no longer present in Fig. 5, and the standard deviation of the residuals is reduced from about 200 mHz to 3.8 mHz by the despinning process. If the estimate of the frequency was slightly off, or if the frequency changed a small amount during the data arc, the residuals would show a clear pattern resulting from the sinusoid of one frequency being subtracting from a sinusoid of a different frequency.

Figure 6 is a plot of the despun residuals vs. phase angle of the spacecraft antenna for the medium gain antenna (MGA). In contrast to the LGA plot in Fig. 3, the MGA does not show a discernible pattern.

Figure 7 shows a histogram of the despun residual values. This is used to gauge roughly how well the residuals fit a Gaussian distribution. The dotted line is the probability distribution function of a Gaussian distribution with the data’s sample mean and variance. Clearly, the residuals are nearly Gaussian, indicating the absence of non-random error sources such as antenna motion. (This analysis could also be done with a Q-Q plot.)

Figure 8 shows the peak frequency vs. time, like in Fig. 2. This plot was a useful diagnostic in case of a pass not being despun properly. Occasionally, MSL performed heat rejection system (HRS)

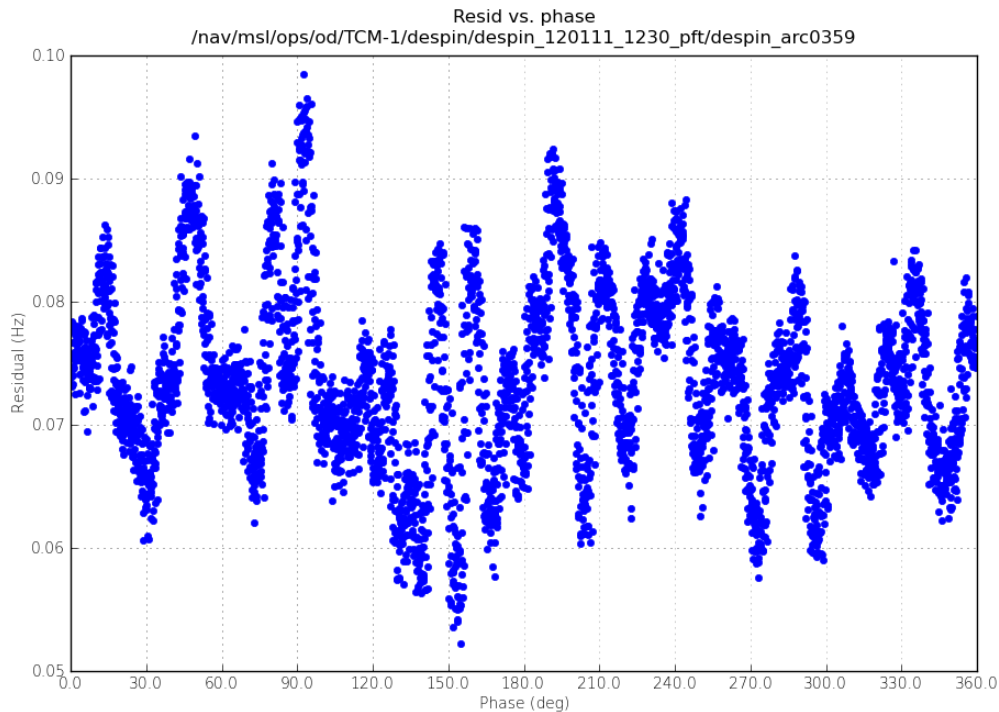


Figure 3: Launch LGA despun residuals vs. spacecraft phase, including Doppler bias

maintenance activities which involved circulating cooling fluid through loops in the spacecraft. This fluid motion changed the spin rate of the spacecraft by about 1 millidegree/second, which is enough that breakpoints were necessary in the despin process. The frequency vs. time plots were very useful in giving the qualitative nature of the spin rate over the pass, as well as the times at which to place the breakpoints. A representative plot from the automated quicklook despin is shown in Fig. 9. The HRS maintenance starts shortly after 19:00 UTC, and continues for about one hour. At that time, one HRS pump was shut down and another was started and left to run for another hour. Shortly after 21:00 UTC, the second pump was turned off and the spacecraft returned to its initial spin rate.

UNPLANNED BENEFITS OF DESPINNING

Although the main purpose of despinning was to produce accurate radiometric data for OD, the despinning process had many other interesting benefits. Most importantly, despinning gave an accurate estimate of the angle between the MSL spin axis and the receiving station on Earth. Also, despinning was used as an independent confirmation of spacecraft clock correlation.

Attitude Estimation

For a period of time after launch, MSL was in a mode where the star trackers had not yet been activated onboard the spacecraft. The only explicit attitude sensors during that time were the sun sensors, which gave the angle between the spin axis and the Sun. When the sun sensor data was combined with the Earth-angle estimate from despinning, the full attitude was estimated with enough accuracy to perform the first (and largest) trajectory correction maneuver. Despinning therefore was a critical part of both the navigation and attitude estimation for the project.

Table 2: Despin filter *a posteriori* sigmas

Parameter	<i>A posteriori</i> sigma
Inertia Frame / W[0]	22.6 deg
Inertia Frame / W[1]	1.09×10^{-2} deg/sec
Inertia Frame / W[2]	2.95×10^{-9} deg/sec ²
Inertia Frame / RA[0]	23.0 deg
Inertia Frame / RA[1]	1.09×10^{-2} deg/sec
Inertia Frame / RA[2]	2.95×10^{-9} deg/sec ²
Inertia Frame / DEC[0]	8.3204484×10^{-3} deg
DSN Two-way Doppler Bias	2.76×10^{-4} Hz
Antenna Cylindrical Radius	4.998×10^{-3} m
Pole Frame / RA[0]	0.528 deg
Pole Frame / DEC[0]	1.73 deg

During the final approach to Mars, the OD team processed over a week of data with no propulsive events in one filter run by manually defining all data to belong to the same data arc. The large time span resulted in a significant change in the Earth-MSL geometry, thereby making the inertial spin axis orientation (pole RA and DEC) fully observable, not just the Earth-angle. This information served as an independent confirmation of the Attitude Control System (ACS) team’s attitude telemetry. For MSL, this was especially important because the attitude knowledge error mapped directly into landing location error. The reported *a posteriori* sigmas values from the OD filter for the Pole Frame / RA[0] were 5.69×10^{-4} deg, and 7.88×10^{-4} deg for Pole Frame / DEC[0]. Compared to the uncertainties obtained during a typical 8-hour pass, such as in Table 2, this long-duration despin decreased attitude uncertainty by about three orders of magnitude.

Spacecraft Clock Calibration

Another major benefit of accurate despining was an independent confirmation of the method used to correlate the on-board spacecraft clock and spacecraft ephemeris time. Accurate timing onboard MSL is critical because of the automated guidance system during entry. Small timing errors in events correspond to large down-track position errors.

During normal operations, we *estimated* the spin state of MSL using Doppler data, which is time-tagged very accurately by the DSN. An alternative approach is to use ACS telemetry to *define* the spin state. Spacecraft telemetry values were accurate enough to support this, but this required downlink of high-rate ACS telemetry, which was not routinely possible due to the low available data rates. Furthermore, there is uncertainty in the time tag of the telemetry measurements.

Fortunately, this presents an opportunity to perform timing correlation by searching for a telemetry timetag offset that minimizes the RMS of the despun residuals, where the despining is accomplished by defining the spin state from telemetry. We computed the despun residuals for various values of a time tag offset, and obtained the RMS of residuals as a function of the time offset. The value of time offset that minimizes the RMS of residuals is the best offset. This offset should be small if the spacecraft clock correlation procedures are working properly, which was verified by this procedure. By performing this offset search over an 8-hour pass, the spacecraft clock correlation was verified to within 0.01 seconds, confirming the correctness of the spacecraft team’s correlation method.

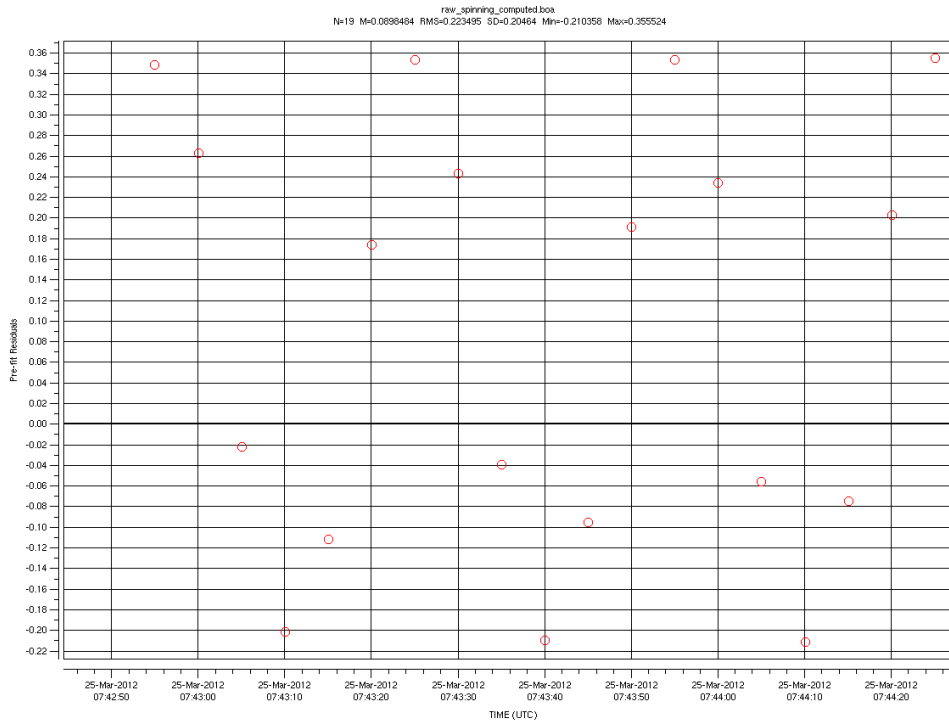


Figure 4: Spinning residuals vs. time

CONCLUSION

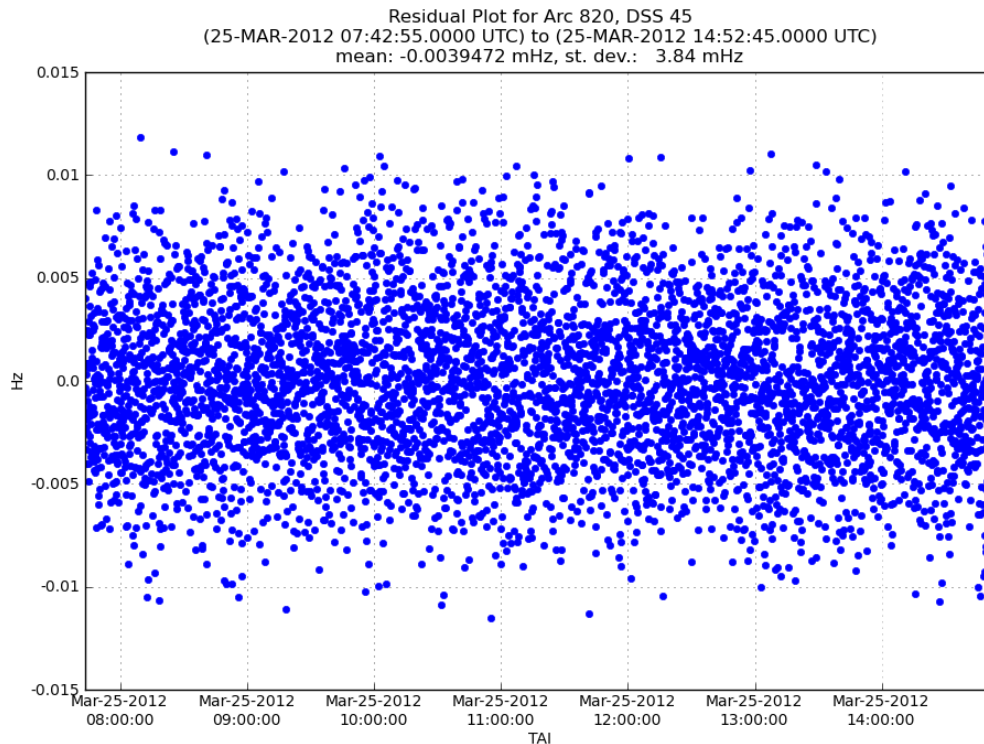
Tools and procedures were developed to properly handle the radiometric tracking data from MSL’s rotating antennas during cruise. This tracking data enabled the mission’s successful navigation. The Juno mission also used these tools with success. There were several unplanned benefits of despinning that helped the project beyond navigation, including attitude estimation and clock correlation. During MSL’s eight-and-a-half-month cruise to Mars, all DSN passes were successfully despun.

ACKNOWLEDGEMENTS

During the hectic first pass after MSL launched, the OD team had two dedicated “despinners”: Matthew Abrahamson and Shadan Ardalan. We thank them both for their excellent support. We also wish to thank Teresa Thomas with Radio-Metric Data Conditioning for her fast and flexible delivery of the tracking data during that period. Last, but not least, we thank the rest of the OD team for their continued feedback and development of the tools: David Jefferson, Neil Mottinger, Frederic Pelletier, Mark Ryne, and Paul Thompson.

This research was carried out at the Jet Propulsion Laboratory, California Institute of Technology, under a contract with the National Aeronautics and Space Administration. Reference herein to any specific commercial product, process or service by trade name, trademark, manufacturer, or otherwise, does not constitute or imply its endorsement by the United States Government or the Jet Propulsion Laboratory, California Institute of Technology.

© 2013 California Institute of Technology. Government sponsorship acknowledged.



REFERENCES

- [1] B. Portock, D. Baird, E. Graat, J. Guinn, T. McElrath, and M. Watkins, "Mars Exploration Rover Cruise Orbit Determination," AIAA/AAS Astrodynamics Specialist Conference and Exhibit, Providence, Rhode Island, USA, 2004.
- [2] D. Han, G. Lewis, G. Wawrzyniak, E. Graat, D. Baird, , and D. Craig, "Genesis Orbit Determination for Earth Return and Atmospheric Entry," 15th AAS/AIAA Space Flight Mechanics Meeting, Copper Mountain, Colorado, USA, 2005.
- [3] L. Cangahuala, E. Graat, D. Roth, S. Demcak, P. Esposito, and R. Mase, "Mars Observer Interplanetary Cruise Orbit Determination," AIAA Space Flight Mechanics Meeting, Cocoa Beach, Florida, USA, 1994.
- [4] T. J. Martin-Mur, G. L. Kruizinga, P. D. Burkhart, M. C. Wong, and F. Abilleira, "Mars Science Laboratory Navigation Results," 23rd International Symposium on Space Flight Dynamics, Pasadena, California, USA, 2012.
- [5] G. L. Kruizinga, E. D. Gustafson, P. F. Thompson, D. C. Jefferson, T. J. Martin-Mur, N. A. Mottinger, F. J. Pelletier, and M. S. Ryne, "Mars Science Laboratory Orbit Determination," 23rd International Symposium on Space Flight Dynamics, Pasadena, California, USA, 2012.
- [6] N. C. Ham, "Helios Spin-Modulation Doppler Effects," *The Deep Space Network Progress Report*, Vol. 42-23, July and August 1974, pp. 87–91.
- [7] R. F. Sunseri, H.-C. Wu, S. E. Evans, J. R. Evans, T. R. Drain, and M. M. Guevara, "Mission Analysis, Operations, and Navigation Toolkit Environment (Monte) Version 040," *NASA Tech Briefs*, Vol. 45, September 2012.
- [8] T. J. Martin-Mur, "Spacecraft Spin Estimation and Spin Signature Removal Using Monte," JPL Inter-Office Memorandum 343A-09-001, Pasadena, California, USA, 2010.
- [9] R. Mackenzie and W. M. Folkner, "Applying Appropriate Weights to Doppler Data," JPL Inter-Office Memorandum 343J-06-034, Pasadena, California, USA, 2006.
- [10] *Numerical Recipes: The Art of Scientific Computing*. New York, New York: Cambridge University Press, 3rd ed., 2007.

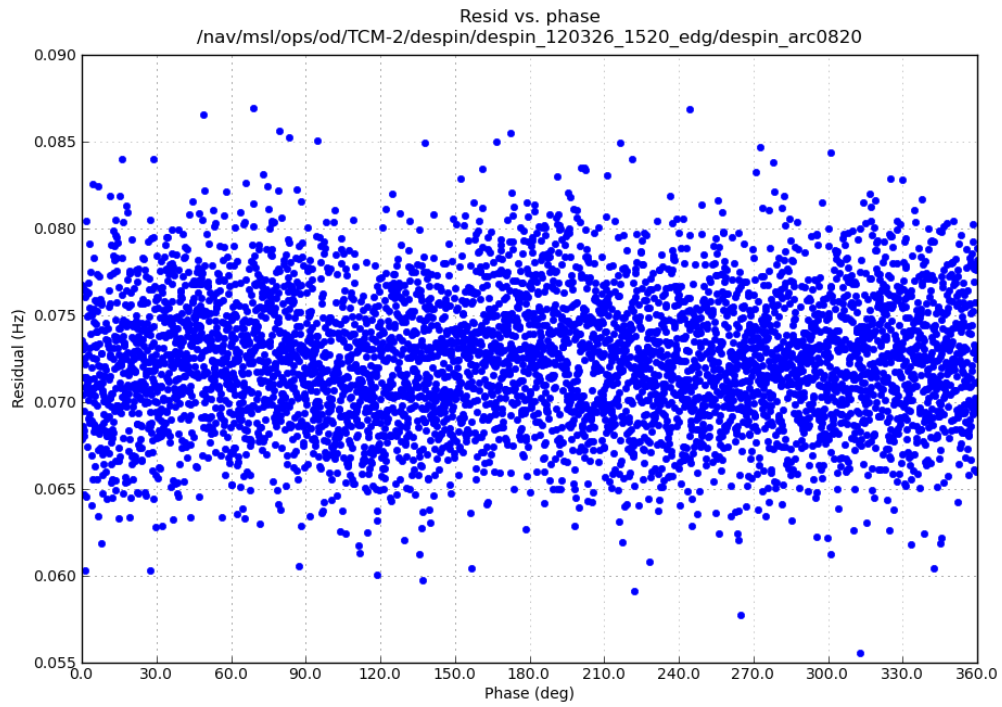


Figure 6: Cruise MGA despin residuals vs. spacecraft phase, including Doppler bias

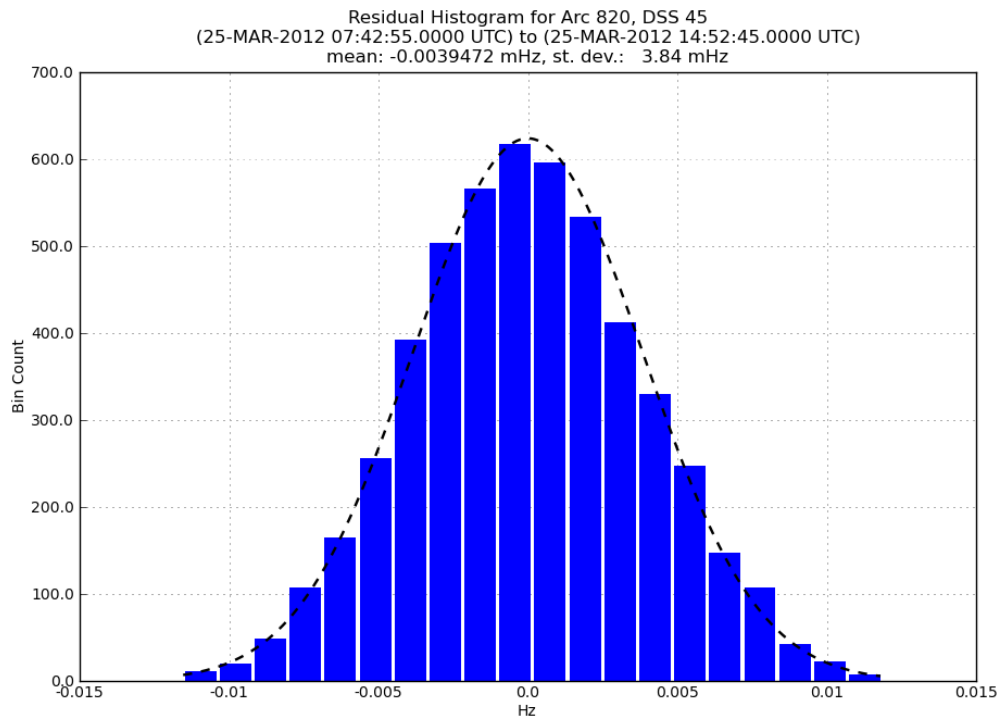


Figure 7: Despin residuals histogram

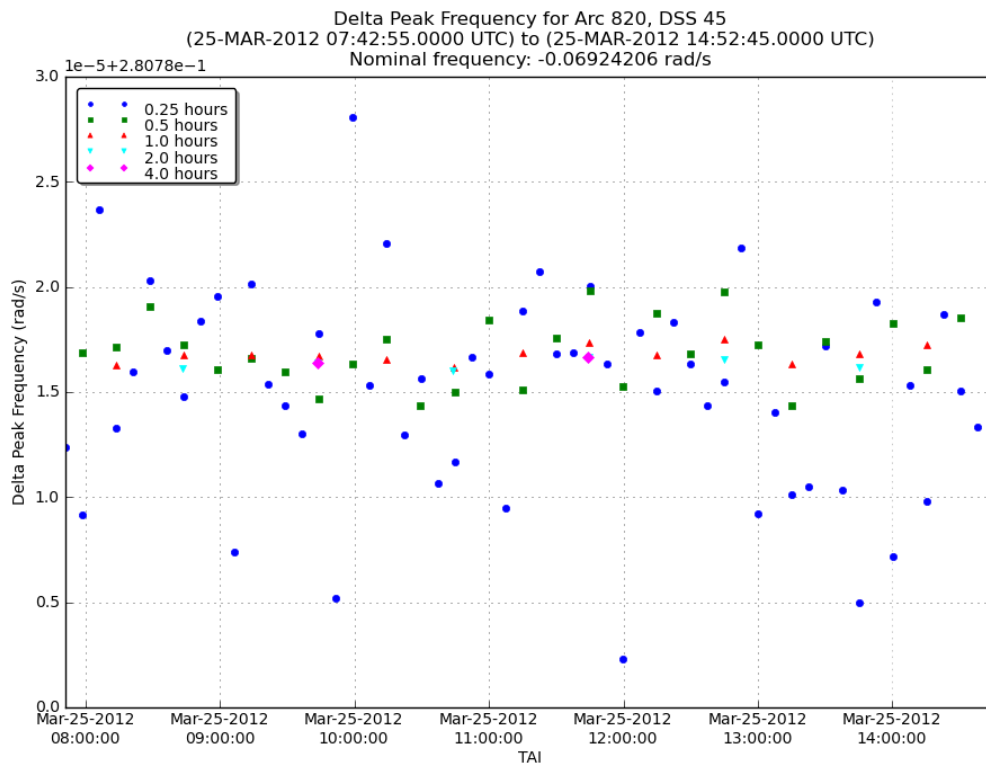


Figure 8: Frequency vs. time

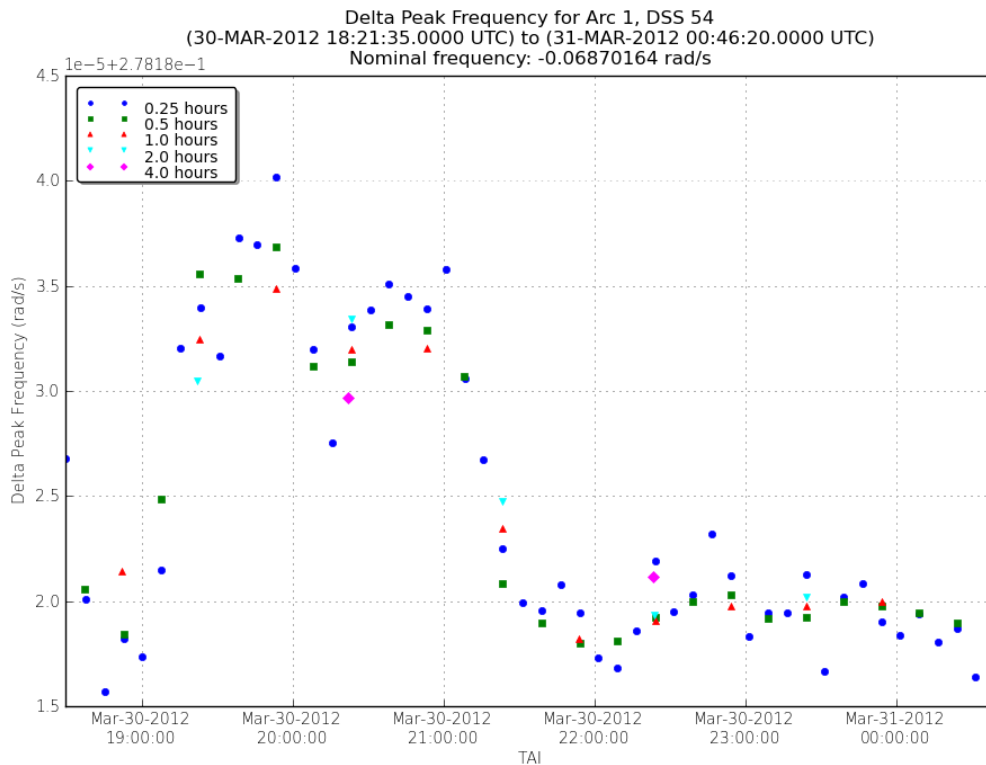


Figure 9: Frequency vs. time during HRS maintenance